Applied Physics Letters

Origin of antiphase domain boundaries and their effect on the dielectric constant of $Ba_{0.5}Sr_{0.5}TiO_3$ films grown on MgO substrates

Cite as: Appl. Phys. Lett. **81**, 4398 (2002); https://doi.org/10.1063/1.1523632
Submitted: 18 June 2002 . Accepted: 30 September 2002 . Published Online: 25 November 2002

Hao Li, H. Zheng, L. Salamanca-Riba, R. Ramesh, I. Naumov, and K. Rabe

Origin of antiphase domain boundaries and their effect on the dielectric constant of $Ba_{0.5}Sr_{0.5}TiO_3$ films grown on MgO substrates

Hao Li, H. Zheng, L. Salamanca-Riba,[a] and R. Ramesh
Materials Science and Engineering Department, University of Maryland, College Park, Maryland 20742

I. Naumov and K. Rabe
Department of Physics and Astronomy, Rutgers University, Piscataway, New Jersey 08854

(Received 18 June 2002; accepted 30 September 2002)

Epitaxial $Ba_{1-x}Sr_xTiO_3$ (BST) with $x=0.5$ films were grown on MgO substrates using pulsed-laser deposition. We have observed a high density of antiphase domain boundaries (ADB) in these BST films. We attribute the formation of the ADBs to the different crystal symmetry of the film and the substrate. Adjacent domains have an in plane phase shift of $\frac{1}{2}[110]$, or $\frac{1}{2}[1\bar{1}0]$ thus creating a phase shift of the in plane lattice planes of $\frac{1}{2}[010]$ or $\frac{1}{2}[100]$ across the boundary. We have used first-principles calculations to obtain the effect of the ADBs on the dielectric constant of $SrTiO_3$ and found that they lower the effective in plane dielectric constant in the direction normal to the ADB. Upon annealing, the density of ADBs decreases and the dielectric properties improve. © *2002 American Institute of Physics.* [DOI: 10.1063/1.1523632]

$Ba_xSr_{1-x}TiO_3$ (BST)-based ceramic thin films are considered by many as the forerunners for room temperature applications of frequency-agile microwave electronic components, including phase shifters, varactors, tunable filters, and antennas.[1–3] BST exhibits a large permittivity, ε_r, that can be as high as 10 000 for bulk samples near the ferroelectric-paraelectric transition temperature (T_c) and can be tuned significantly with an applied electric field. However, compared to bulk BST samples, ε_r and its tunability, of epitaxial thin films (<300 nm thick) are markedly lower ($\varepsilon_r<3500$). Large values of the peak ε_r (near T_c) of 4130 before annealing and 6020 after annealing at $V=0$ have been reported in BST films with thickness of 500 nm.[4] The increase in ε_r upon annealing was associated with strain relaxation of the lattice. Strain and defects are considered two primary causes for the degradation of the dielectric properties of BST thin films.[5–7] Annealing of the BST films leads to partial recovery in their dielectric properties.[8,9] This enhancement has been attributed to the relief of macrostress in the BST thin films.[10] We have previously presented systematic studies of the effect of strain on the dielectric properties of BST thin films.[11,12] X-ray diffraction analysis of our BST films did not show an appreciable change of the lattice constants upon annealing, indicating that annealing did not change the macrostress state of the BST thin films. We attribute the increase in ε_r upon annealing to a reduction of defects present in the BST films. Particularly, we have found that antiphase domain boundaries (ADB) exist in BST films grown on substrates having different crystal symmetry (other than perovskite). Jiang *et al.*[13] have recently reported the formation of ADBs in BST films grown on MgO substrates that result from steps and kinks on the surface of the MgO substrate and the observation that TiO_2 is the first layer that grows on the substrate. In the present work we report another mechanism for the formation of ADBs in BST films grown on flat surfaces of MgO that results solely from the different structure of BST (perovskite) and MgO (rock salt). We also present the atomic morphology of the ADBs and their effect on the dielectric properties of BST thin films.

We have grown 100 nm thick BST ($x=0.5$) thin films on (001) MgO substrates using a 248 nm excimer pulsed laser deposition system. The substrate temperature was held at 800 °C for all samples. A dynamic pressure of 120 mTorr O_2 was established in the chamber during deposition and the samples were cooled down under 700 Torr O_2 after deposition. The laser fluence was ~ 1.5 J/cm^2, corresponding to a growth rate of 0.08 nm/s. Annealing experiments were carried out at 950 °C for 14 h in a quartz tube in flowing oxygen ambient. Dielectric measurements were performed using the conventional interdigital electrode method consisting of 50 fingers separated by 15 μm gaps. Each finger had a width of 25 μm and length of 0.70 cm. The dielectric properties were then measured using an HP 4192 impedance/gain analyzer. The permittivity of the BST films was extracted from the capacitance data using Gevorgian *et al.* model.[14] Transmission electron microscopy (TEM) analysis was done using a JEOL 4000 FX (TEM) operated at 300 kV and a JEOL 4000 EX TEM operated at 400 kV. TEM samples were prepared by mechanical polishing at high angles down to electron transparency using a quadripod.[15]

The RT in plane dielectric constant, ε_{11} of the BST films as a function of applied voltage before and after annealing showed a maximum value of (at ~ 0 V and RT) of 1920 in the as-grown samples and 2460 in the annealed samples. Both of these values are much lower than the value of ε_{11} in bulk BST that is ~ 6000 for the composition studied in this work. Figure 1 shows bright field plan-view images from a BST sample before and after annealing. The images show domains (arrowed) with an average width of ~ 40 nm before annealing and 120 nm after annealing. The domains are identified as antiphase domains as can be seen in the high-resolution lattice image of one of the boundaries in Fig. 2. This image clearly shows a shift in the (100) atomic planes across the ADB by $\frac{1}{2}[100]$. A comparison of the image with simulated images indicates that the ADB consists of a double

[a]Electronic mail: riba@eng.umd.edu

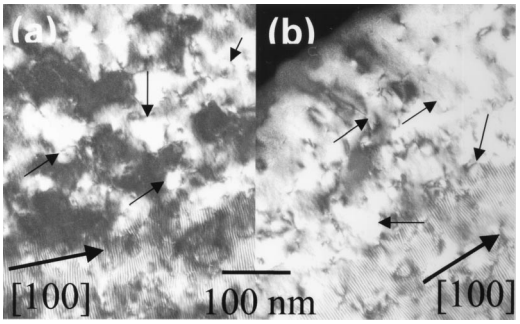

FIG. 1. Plan-view bright-field images of (a) as-deposited and (b) annealed BST film on MgO showing ADBS (arrowed). The bottom part of the images also show Moire fringes due to the overlap of the BST and MgO in thicker parts of the sample. The Moire fringes indicate that the film is relaxed.

layer of Ba/SrO. We also observed ADBs consisting of double layers of TiO_2.

There are two possibilities for ADBs to form in epitaxial BST films. In the first configuration, the phase shift is perpendicular to the interface and the two antiphase domains have a relative shift of $\frac{1}{2}[001]$ along the *c* axis (normal) of the film. A possible formation of these ADBs could result from adjacent nuclei having different layers in the BST as the first layer deposited on MgO. As shown later this is not a possible configuration for BST. Another possibility for the formation of this kind of ADBs was previously discussed for the case of BST films as resulting from steps of half a unit cell height $\frac{1}{2}a_{MgO}$ on the Mgo substrate (conservative ADB).[13]

The second configuration of ADBs corresponds to in plane shifts (either $\frac{1}{2}[100]$ or $\frac{1}{2}[010]$) of the lattice planes from one domain to the next. Some possible causes of in-plane ADB formation were also described by Jiang *et al.*[13] In this case, terraces with widths equal to an odd multiple of $\frac{1}{2}a_{MgO}$ give rise to nonconservative ADBs. Here we discuss another mechanism for the formation of ADBs with in plane shift between domains that can take place even on a flat surface of MgO. We begin by discussing the possible nucleation configurations of BST on MgO. MgO has a rock salt structure with a (001) surface as shown in Fig. 3(a). In contrast, BST has a perovskite structure with alternating $Ba_{1-x}Sr_xO$ and TiO_2 layers along the $\langle 001 \rangle$ direction as shown in Figs. 3(b) and 3(c), respectively. Since the interface between two ionic crystals has the lowest energy if the nearest neighbor ions across the interface have charges of opposite sign we should consider which layer is the most likely

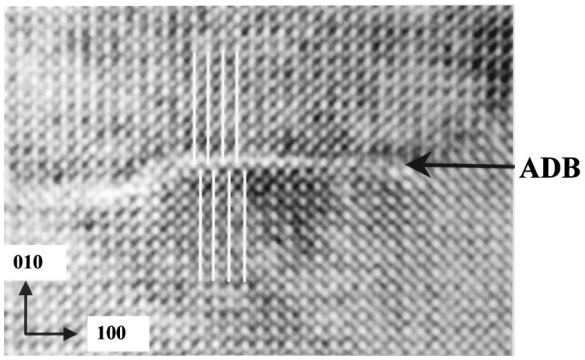

FIG. 2. Plan-view high-resolution image of a BST film showing an ADB. The ADB is a Ba/SrO double layer.

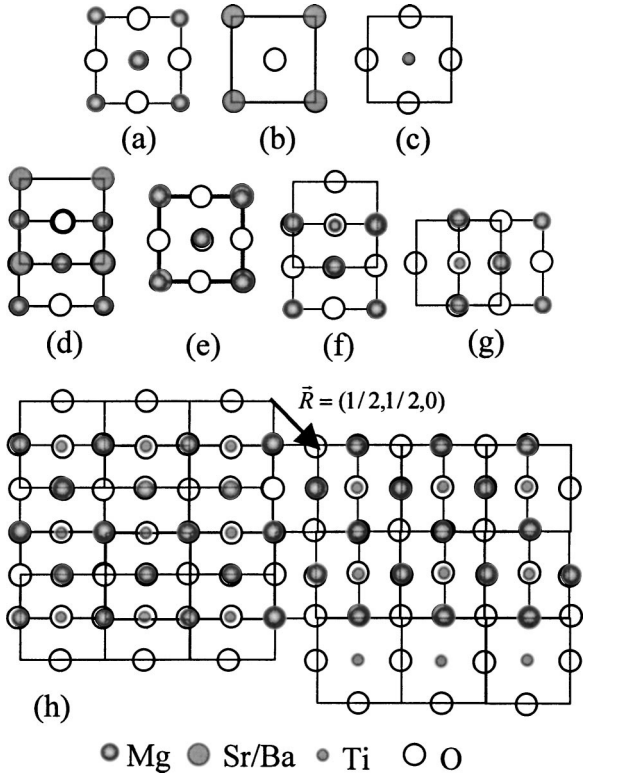

FIG. 3. Schematic of (a) (001) surface of MgO, (b) (BaSrO) layer of BST, (c) (TiO_2) layer of BST, (d) stacking sequence of (Ba,Sr)O on MgO where O ions sit on top of each other, (e) stacking sequence of (Ba,Sr)O on MgO where cations sit on top of each other, (f) stacking sequence of TiO_2 on MgO (I), (g) stacking sequence of TiO_2 on MgO (II), and (h) boundary between two TiO_2 variants grown on MgO.

layer to grow on MgO first. If (BaSrO) nucleates first on MgO, this condition cannot be satisfied as can be seen from Fig. 3. Namely, either the anions (oxygen ions) [Fig. 3(d)] or the cations (Mg and Sr/Ba) become nearest neighbors [Fig. 3(e)]. In contrast, if the TiO_2 nucleates first on MgO the bonding for both anions and cations can be satisfied without any conflict [Fig. 3(f)]. Thus, it is energetically more favorable for the TiO_2 layer to nucleate first on the MgO substrate. This type of interface has already been observed in other materials with perovskite structure grown on MgO first.[16–18] Since the stacking sequence is determined, ADBs with a $\frac{1}{2}[001]$ shift are not likely to form in BST films on flat surfaces of MgO substrates. In fact, we did not observe any ADBs of this type in our TEM studies.

The ADBs with in-plane shift form because there are two possibilities (variants) for the TiO_2 layer to stack on the (001) surface of MgO that are equally possible as shown in Figs. 3(f) and 3(g). Both types of stacking have exactly the same neighbors for each ion across the interface but they have a relative in plane shift of $\mathbf{R} = \frac{1}{2}[110]$. Therefore, when two nuclei with different variant of the TiO_2 atomic arrangement meet during the growth of the film, an ADB with a phase shift of the lattice planes of $\frac{1}{2}[010]$ or $\frac{1}{2}[100]$ forms at the plane where the domains meet. Since both domains are equally possible to form during nucleation, it is very likely for BST films to have this type of ADBs even on flat MgO surfaces. Figure 3(h) shows a schematic of the TiO_2 layer after two domains meet. The domain boundary in this layer contains two rows of oxygen (one in each domain). However, when the second (Ba/SrO) layer is deposited the bound-

ary will contain a double layer of Ba/Sr atoms. Therefore, as the film growth progresses the boundary will contain a double layer of Ba/SrO. Similarly, a relative shift of $\mathbf{R}=1/2[1\bar{1}0]$ between domains gives rise to a TiO_2 double layer at the boundary. To keep the overall stoichiometry, the ADBs alternate from Sr/BaO to TiO_2.

To gain insight into the structural energetics of the ADBs and their effects on ϵ_r, we have performed a first-principles study of pure bulk $SrTiO_3$ with a periodic array of infinite planar ADBs separated by $3a$ (three unit cells of $SrTiO_3$). Using ABINIT, a pseudopotential implementation of variational density functional perturbation theory,[19] we have investigated changes in the structure, total energy, lattice dynamics and dielectric properties due to the introduction of two different ADBs (Sr-rich and Ti-rich). Both types of ADBs are found to produce considerable compressive stress perpendicular to the interface plane. After optimizing the energy to find the equilibrium atomic positions, we calculated the infrared-active phonon frequencies ω_λ and effective Born charge tensor $Z^*_{\kappa,\alpha\beta}$ for each atom κ; these quantities determine the static dielectric tensor $\varepsilon_{\alpha\beta}$ through the relation

$$\varepsilon_{\alpha\beta}=\varepsilon^{\infty}_{\alpha\beta}+\frac{4\pi}{\Omega}\sum_{\lambda} S_{\lambda,\alpha\beta}/\omega^2_{\lambda},$$

where $S_{\lambda,\alpha\beta}=[\sum_{\kappa,\gamma} Z^*_{\kappa,\alpha\gamma}U_\lambda(\kappa,\gamma)]\times[\sum_{\kappa',\delta} Z^*_{\kappa',\beta\delta}U_\lambda(\kappa',\delta)]$ is the mode oscillator strength tensor, $U_\lambda(\kappa,\gamma)$ are the eigendisplacements of the force constant matrix, $\varepsilon^{\infty}_{\alpha\beta}$ is the dielectric constant at high frequency, and Ω is the unit cell volume. Comparing with the dielectric response of ideal $SrTiO_3$, we find that the dielectric response perpendicular to the ADBs, ε_{zz}, is greatly reduced (see Table I). This reduction can be directly attributed to the breaking of the infinite Ti–O chains normal to the ADBs. So, though the spacing of the ADBs in the supercell is much smaller than in the films studied, the calculations provide physical understanding of the local changes in interatomic force constants that impact the dielectric constant $\varepsilon_{\alpha\beta}$.

In the experimentally studied BST films, the analogous disruption of the Ti–O chains should lead to a similar local reduction of the dielectric response. Since the system is at a temperature just above the ferroelectric transition, the effects of the disruption propagate into a region with characteristic size equal to the Landau correlation length ξ and thus, despite the low density of ADBs, significantly contribute to the observed reduction in ϵ_r. An estimate for ξ can be obtained from the Ginzburg–Landau free energy density[20]

$$F=\tfrac{1}{2}AP^2+\tfrac{1}{4}BP^4+\tfrac{1}{6}CP^6+\tfrac{1}{2}D(\nabla P)^2-EP,$$

where $A\equiv\chi^{-1}$, $D\equiv 2\xi_0^2$, χ is the local susceptibility, ξ_0 is the persistence length, E and P are the applied electric field and the polarization, respectively, and B and C are constants. ξ is defined by $(D/A)^{1/2}\equiv(2\chi)^{1/2}\xi_0$, and $\varepsilon=1+4\pi\ \chi$ ($\varepsilon\cong 10^4$ for BST), and $\chi\cong 10^3$. The estimated value of D for $BaTiO_3$ is $1.14\times10^{-7}\ \mathrm{J\,m^3C^{-2}}$ or simply $0.12\times10^{-16}\ \mathrm{m^2}$.[20] Using this value for BST we obtain $\xi\sim 10^2$ nm.

After annealing the size of the antiphase domains increases (see Fig. 1), at the same time the dielectric constant increases. Based on our experimental results and our first-principles calculations we believe that the increase in domain size (reduction in density of ADBs) is one of the primary causes for the 28% recovery of the dielectric properties upon annealing.

TABLE I. Electronic, phonon, and total dielectric tensors along the z direction for $SrTiO_3$ with ADBs compared to pure $SrTiO_3$.

ε_{zz}	Pure $SrTiO_3$	SrO ADB	TiO_2 ADB	Mixed ADBs
Electronic	6.2	5.1	6.0	5.4
Phonon	169.8	23.8	40.2	18.3
Total	176.0	28.9	46.2	23.7

In summary, we have observed a high density of ADBs in BST films grown on MgO substrates which form due to the different crystal symmetry of the film and the substrate. Adjacent domains in BST films have an in plane phase shift of $\mathbf{R}=\frac{1}{2}[110]$, or $\mathbf{R}=\frac{1}{2}[1\bar{1}0]$ thus creating ADBs with a phase shift of the lattice planes of $\frac{1}{2}[010]$ or $\frac{1}{2}[100]$ across the ADBs. First-principles calculations indicate that the ADBs lower the dielectric constant of BST because the Ti–O chains are broken across the ADB.

This project was supported by NSF MRSEC under Grant No. DMR 00-80008. The authors thank M. H. Cohen for helpful discussions and C. H. Chen at the University of Virginia for the use of the JEOL 4000 EX TEM.

[1] V. K. Varadan, V. V. Varadan, F. Selmi, Z. Ounaies, and K. A. Jose, Proc. SPIE **2189**, 433 (1994).
[2] F. S. Barnes, J. Price, A. Hermann, Z. Zhang, H.-D. Wu, D. Galt, and A. Naziripour, Integr. Ferroelectr. **8**, 171 (1995).
[3] J. Im, O. Auciello, P. K. Baumann, S. K. Streiffer, D. Y. Kaufman, and A. R. Krauss, Appl. Phys. Lett. **76**, 625 (2000).
[4] C. M. Carlson, T. V. Rivkin, P. A. Parilla, J. D. Perkins, D. S. Ginley, A. B. Kozyrev, V. N. Oshadchy, and A. S. Pavlov, Appl. Phys. Lett. **76**, 1920 (2000).
[5] T. M. Shaw, Z. Suo, M. Huang, E. Liniger, R. B. Laibowitz, and J. D. Baniecki, Appl. Phys. Lett. **75**, 2129 (1999).
[6] L. Ryen, E. Olsson, L. D. Madsen, C. N. L. Edvardsson, X. Wang, S. N. Jacobsen, U. Helmersson, S. Rudner, and L. D. Wernlund, J. Appl. Phys. **83**, 4884 (1998).
[7] W. Chang, C. M. Gilmore, W. J. Kim, J. M. Pond, S. W. Kirchoefer, S. B. Qadri, D. B. Chrisey, and J. S. Horwitz, J. Appl. Phys. **87**, 3044 (2000).
[8] W. Chang, J. S. Horwitz, A. C. Carter, J. M. Pond, S. W. Kirchoefer, C. M. Gilmore, and D. B. Chrisey, Appl. Phys. Lett. **74**, 1033 (1999).
[9] L. A. Knauss, J. M. Pond, J. S. Horwitz, D. B. Chrisey, C. H. Mueller, and R. Treece, Appl. Phys. Lett. **69**, 25 (1996).
[10] J. S. Horwitz, W. Chang, W. Kim, S. B. Qadri, J. M. Pond, S. W. Kirchoefer, and D. B. Chrisey, J. Electroceram. **4**, 357 (2000).
[11] C. L. Canedy, H. Li, S. P. Alpay, L. Salamanca-Riba, A. L. Roytburd, and R. Ramesh, Appl. Phys. Lett. **77**, 1695 (2000).
[12] H. Li, A. L. Roytburd, S. P. Alpay, T. D. Tran, L. Salamanca-Riba, and R. Ramesh, Appl. Phys. Lett. **78**, 2354 (2001).
[13] J. C. Jiang, Y. Lin, C. L. Chien, C. W. Chu, and E. I. Meletis, J. Appl. Phys. **91**, 3188 (2002).
[14] S. S. Gevorgian, T. Martinsson, P. L. J. Linner, and E. L. Kollberg, IEEE Trans. Microwave Theory Tech. **44**, 896 (1996).
[15] H. Li and L. Salamanca-Riba, Ultramicroscopy **88**, 171 (2001).
[16] S. Hsien Rou, T. M. Graettinger, O. Auciello, and A. I. Z. A. Kingon, Heteroepitaxy of Dissimilar Materials Symposium 1991, pp. xv+504, 65–70.
[17] H. W. Zandbergen, J. G. Wen, C. Traeholt, and V. Svetchnikov, J. Alloys Compd. **195**, 85 (1993).
[18] C. Traeholt, J. G. Wen, V. Svetchnikov, and H. W. Zandbergen, Physica C **230**, 297 (1994).
[19] ABINIT code is a common project of the Universite Catholique de Louvain, Corning Incorporated, and other contributors (URL http://www.abinit.org) (1999-2002).
[20] C. L. Wang and S. R. Smith, J. Phys.: Condens. Matter **7**, 7163 (1995).